

On the Approximation Quality of Markov State Models*

Marco Sarich**¹, Frank Noé***¹, and Christof Schütte^{†1}

¹ Institut für Mathematik II, Freie Universität Berlin
Arnimallee 2-6, 14195 Berlin, Germany

Key words Markov state model, biomolecular dynamics conformations, metastable sets, effective dynamics, transfer operator, spectral gap, lag time, diffusive dynamics

Abstract. We consider a continuous-time Markov process on a large continuous or discrete state space. The process is assumed to have strong enough ergodicity properties and exhibit a number of metastable sets. Markov state models (MSM) are designed to represent the effective dynamics of such a process by a Markov chain that jumps between the metastable sets with the transition rates of the original process. MSM are used for a number of applications, including molecular dynamics, since more than a decade. Their approximation quality, however, has not yet been fully understood. In particular, it would be desirable to have a sharp error bound for the difference in propagation of probability densities between the MSM and the original process on long time scales. Here, we provide such a bound for a rather general class of Markov processes ranging from diffusions in energy landscapes to Markov jump processes on large discrete spaces. Furthermore, we discuss how this result puts formal support or shows the limitations of algorithmic strategies that have been found to be useful for the construction of MSMs. Our findings are illustrated by numerical experiments.

This is a preliminary version. Do not circulate!

1 Introduction

We consider a continuous-time Markov process $(X_t)_{t \in \mathbb{R}}$ on some state space E which may be continuous or discrete but large. We assume that the process is sufficiently ergodic in E such that there is a unique invariant measure μ . The associated semi-group of transfer operators is denoted $(T_t)_{t \in \mathbb{R}}$; the transfer operators describe how the process propagates functions in state space, e.g., if v_0 is a function at time $t = 0$ then $T_t v_0$ is the function that results from time- t -transport of v_0 via the underlying dynamics.

Markov state models (MSM) have been considered for processes that have metastable dynamics [1, 2, 3, 4], especially in Molecular Dynamics. Recently the interest in MSMs has drastically increased since it could be demonstrated that MSMs can be constructed even for very high dimensional systems [2] and have been especially useful for modeling the interesting slow dynamics of biomolecules [5, 6, 7, 8, 9, 10] and materials [11] (there under the name "kinetic Monte Carlo"). Their approximation quality on large time scale has been rigorously studied, e.g., for Brownian or Glauber dynamics and Ising models in the limit of vanishing smallness parameters (noise intensity, temperature) where the analysis can be based on large deviation estimates and variational principles [12, 13] and/or potential theory and capacities [14, 15]. In these cases the effective dynamics is governed by some MSM with exponentially small transition probabilities and its states label the different attractors of the underlying, unperturbed dynamical systems. Other approaches tried to understand the multi-dimensional setting for complex dynamical systems by generalization of Kramer's approach, e.g., by discussing asymptotic expansions based on the Wentzel-Kramers-Brillouin approximation in semiclassical quantum dynamics, matched asymptotics or similar techniques, see e.g. [16, 17]. Another rigorous approach to the construction of MSM involves the exploitation of spectral properties. The relation between dominant eigenvalues, exit times and rates, and metastable sets has been studied by asymptotic expansions in certain smallness

* Supported by the DFG research center MATHEON "Mathematics for key technologies" in Berlin.

** E-mail: sarich@math.fu-berlin.de

*** E-mail: noe@math.fu-berlin.de

† E-mail: schuette@math.fu-berlin.de

parameters as well as by functional analytic means without any relation to smallness parameters [18, 19, 3, 4, 1]. In real applications with high-dimensional state spaces asymptotic expansions are based on assumptions that typically cannot be checked and often enough are not satisfied, involve quantities that cannot be computed, and/or are rather specific for a certain class of processes. Even if a smallness parameter can be defined we typically cannot check whether we are in the asymptotic regime such that the theoretical results cannot be used for error estimates. A general approach for accessing the approximation quality of a MSM is still missing. Here, we will pursue this by following the functional analytic approach found in [20, 19, 3].

In order to explain the construction of a MSM, we first fix a lag time $\tau > 0$ and consider some finite subdivision A_1, \dots, A_n of E , such that

$$\bigcup_{j=1}^n A_j = E \quad A_i \cap A_j = \emptyset \quad \forall i \neq j, \quad (1)$$

with “nice” sets A_j (e.g. with Lipschitz boundary). We introduce the discrete process $(\hat{X}_k)_{k \in \mathbf{N}}$ on the finite state space $\hat{E} = \{1, \dots, n\}$ by setting

$$\hat{X}_k = i \Leftrightarrow X_{k\tau} \in A_i. \quad (2)$$

(\hat{X}_k) describes the snapshot dynamics of the continuous process (X_t) with lag time τ between the sets A_1, \dots, A_n . This process (\hat{X}_k) is generally not Markovian, i.e.

$$\mathbb{P}[\hat{X}_{k+1} = j | \hat{X}_k = i_k, \hat{X}_{k-1} = i_{k-1}, \dots, \hat{X}_0 = i_0] \neq \mathbb{P}[\hat{X}_{k+1} = j | \hat{X}_k = i_k]. \quad (3)$$

However, MSMs attempt to approximate this process *via* a discrete Markov process $(\tilde{X}_k)_{k \in \mathbf{N}}$ on $\hat{E} = \{1, \dots, n\}$ defined by the transition matrix P with entries

$$P_{ij} = \mathbb{P}_\mu[\hat{X}_1 = j | \hat{X}_0 = i] = \mathbb{P}_\mu[X_\tau \in A_j | X_0 \in A_i]. \quad (4)$$

While the long-term dynamical behavior of the original process $(X_{k\tau})_{k \in \mathbf{N}}$ is governed by $T_{k\tau} = T_\tau^k$ for $k \in \mathbf{N}$, the long-term dynamics of the MSM process $(\tilde{X}_k)_{k \in \mathbf{N}}$ is governed by P^k . Thus, for accessing the approximation quality of the Markov state model compared to the original process, we have to study the error (use subscript τ either for both T and P or none.)

$$E(k) = \text{dist}(T_\tau^k, P^k),$$

where dist denotes an appropriate metric measuring the difference between the operators. We will see that under strong enough ergodicity conditions on the original Markov chain, we have $E(k) \leq 2\rho^k$ for some $0 < \rho < 1$. However, we are interested in how $E(k)$ depends on the lag time τ and the sets A_1, \dots, A_n such that the error E can be kept below a user-defined threshold.

The remainder of the article is organized as follows. In Section 2 we introduce the setting and give the general definition of MSM transfer operators. Then, in Sec. 3 we compare the densities of the random variables (\hat{X}_k) to the densities of the MSM process (\tilde{X}_k) and see, how the approximation quality of these densities depends on the choice of the state space discretization A_1, \dots, A_n and the lag time τ . Section 4 extends our findings to some algorithmic strategies for the construction of MSMs that are discussed in the literature. Finally, the results are illustrated on numerical examples in Section 5.

2 The MSM transfer operator

2.1 Setting

We consider the transfer operators T_t as operators on $L_\mu^2 = \{v : E \rightarrow \mathbf{R} : \int v^2 d\mu < \infty\}$ with scalar product $\langle v, w \rangle = \int v w d\mu$. In the following $\|\cdot\|$ will denote the associated norm $\|v\|^2 = \langle v, v \rangle$ on L_μ^2 and the corresponding operator norm $\|B\| = \max_{\|v\|=1} \|Bv\|$ of an operator $B : L_\mu^2 \rightarrow L_\mu^2$.

In L^2_μ , T_τ has the general form

$$\int_C T_\tau v(x) \mu(dx) = \int \mathbb{P}[X_\tau \in C | X_0 = x] v(x) \mu(dx), \quad \text{for all measurable } C \subset E,$$

such that $T_\tau \mathbf{1} = \mathbf{1}$ where $\mathbf{1}(x) = 1$ for all $x \in E$. In the following we set $T := T_\tau$.

2.2 Assumptions on the original process

Now let us assume that T has m real eigenvalues $\lambda_1, \dots, \lambda_m \in \mathbb{R}$

$$\lambda_0 = 1 > \lambda_1 \geq \lambda_2 \geq \dots \geq \lambda_m, \quad (5)$$

with an orthonormal system of eigenvectors $(u_j)_{j=1, \dots, m}$, i.e.

$$T u_j = \lambda_j u_j, \quad \langle u_i, u_j \rangle = \begin{cases} 1, & i = j \\ 0, & i \neq j \end{cases} \quad (6)$$

and $u_0 = \mathbf{1}$. Furthermore we assume that the remainder of the spectrum of T lies within a ball $B_r(0) \subset \mathbb{C}$ with radius $r < \lambda_m$. In order to keep track of the dependence of the eigenvalues on the lag time τ we introduce the associated rates

$$\lambda_j = \exp(-\Lambda_j \tau), \quad r = \exp(-R\tau), \quad r/\lambda_1 = \exp(-\tau(R - \Lambda_1)) = \exp(-\tau\Delta), \quad (7)$$

of which the *spectral gap* $\Delta > 0$ will play an essential role later on.

Based on the above assumptions we can write

$$T v = T \Pi v + T \Pi^\perp v = \sum_{j=0}^m \lambda_j \langle v, u_j \rangle u_j + T \Pi^\perp v, \quad (8)$$

where Π is the orthogonal projection onto $U = \text{span}\{u_1, \dots, u_m\}$

$$\Pi v = \sum_{j=0}^m \langle v, u_j \rangle u_j \quad (9)$$

and $\Pi^\perp = \text{Id} - \Pi$ is the projection error with

$$\|T \Pi^\perp\| \leq r < \lambda_m, \quad \text{spec}(T) \setminus \{1, \lambda_1, \dots, \lambda_m\} \subset B_r(0) \subset \mathbb{C}. \quad (10)$$

Furthermore, we assume that the subspace U and the remaining subspace don't mix under the action of T :

$$\Pi T \Pi^\perp = \Pi^\perp T \Pi = 0 \quad (11)$$

and therefore the dynamics can be studied by considering the dynamics of both subspaces separately

$$T^k = (T \Pi)^k + (T \Pi^\perp)^k \quad \forall k \geq 0, \quad (12)$$

where the operator $T \Pi$ is self-adjoint because of (6). In addition we also define the orthogonal projection Π_0 as

$$\Pi_0 v := \langle v, u_0 \rangle u_0 = \langle v, \mathbf{1} \rangle \mathbf{1}.$$

According to the above we have the asymptotic convergence rate $\|T^k - \Pi_0\| = \lambda_1^k$ for all $k \in \mathbb{N}$.

Remark 2.1 The assumptions (5), (6), (10), and (11) are definitely satisfied if T is self-adjoint and has strong enough ergodicity properties. T is self-adjoint if the underlying original Markov process (X_t) is reversible. But it may also be sufficient if, e.g., (\tilde{X}_t) has a dominant self-adjoint part as it is the case for second-order Langevin dynamics with not too large friction [21], or for thermostatted Hamiltonian molecular dynamics or stochastically perturbed Hamiltonian systems [3, 22].

2.3 MSM Projection

Let χ_A denote the characteristic function of set A . We define the orthogonal projection Q onto the n dimensional space of step functions $D_n = \text{span}\{\chi_{A_1}, \dots, \chi_{A_n}\}$, i.e.

$$Qv = \sum_{i=1}^n \frac{\langle v, \chi_{A_i} \rangle}{\mu(A_i)} \chi_{A_i} = \sum_{i=1}^n \langle v, \phi_i \rangle \phi_i \quad (13)$$

with orthonormal basis $(\phi_i)_{i=1, \dots, n}$ of D_n

$$\phi_i = \frac{\chi_{A_i}}{\sqrt{\mu(A_i)}}.$$

In short the orthogonal projection Q keeps the measure on the sets A_1, \dots, A_n , but on each of the sets the ensemble will be redistributed according to the invariant measure and the detailed information about the distribution inside of a set A_i is lost.

Since the sets A_1, \dots, A_n form a full partition of E we have

$$Q\mathbf{1} = \mathbf{1}, \quad (14)$$

which implies

$$Q\Pi_0 = \Pi_0 Q = \Pi_0. \quad (15)$$

2.4 MSM transfer operator

Now consider the projection of our transfer operator T onto D_n :

$$P = QTQ : L_\mu^2 \rightarrow D_n \subset L_\mu^2. \quad (16)$$

In order to understand the nature of P let us consider it as an operator on a finite dimensional space, $P : D_n \rightarrow D_n$. Here, as a linear operator on a finite-dimensional space, it has a matrix representation with respect to some basis. Let us take the basis $(\psi_i)_{i=1, \dots, n}$ of probability densities given by

$$\psi_i = \frac{\chi_{A_i}}{\mu(A_i)}. \quad (17)$$

By using the definition of T we get

$$\begin{aligned} P\psi_i &= QTQ\psi_i = QT\psi_i = \sum_{j=1}^n \frac{\langle T\psi_i, \chi_{A_j} \rangle}{\mu(A_j)} \chi_{A_j} = \sum_{j=1}^n \frac{\langle T\chi_{A_i}, \chi_{A_j} \rangle}{\mu(A_i)} \psi_j \\ &= \sum_{j=1}^n \left(\int_{A_i} \mathbb{P}[X_\tau \in A_j | X_0 = x] \mu(dx) \right) \cdot \psi_j. \end{aligned}$$

such that

$$P\psi_i = \sum_{j=1}^n P_\mu[X_\tau \in A_j | X_0 \in A_i] \cdot \psi_j. \quad (18)$$

So the transition matrix of the MSM Markov chain defined in Eq. (4) is identical with the matrix representation for the projected transfer operator P ; therefore P is the MSM transfer operator. P inherits the ergodicity properties and the invariant measure of T as the following lemma shows (the proof can be found in Sec. 6.1 below):

Lemma 2.2 *For every $k \in \mathbb{N}$ we have*

$$\|P^k - \Pi_0\| \leq \|(TQ)^k - \Pi_0\| \leq \lambda_1^k.$$

3 Approximation quality of coarse-grained transfer operators

3.1 Approximation Error E

The approximation quality of the MSM Markov chain can be characterized by comparing the operators P^k and T^k for $k \in \mathbb{N}$ restricted to D_n :

$$E(k) = \|QT^kQ - P^k\| = \|QT^kQ - Q(TQ)^k\|. \quad (19)$$

Lemma 2.2 immediately implies that this error decays exponentially,

$$E(k) = \|QT^kQ - P^k\| \leq \|QT^kQ - \Pi_0\| + \|P^k - \Pi_0\| \leq \|Q(T^k - \Pi_0)Q\| + \|P^k - \Pi_0\| \leq 2\lambda_1^k, \quad (20)$$

independent of the choice of the sets A_1, \dots, A_n . Since we want to understand how the choice of the sets and other parameters like the lag time τ influence the approximation quality we have to analyse the pre-factor in much more detail.

3.2 Main Result: An Upper Bound on E

The following theorem contains the main result of this article:

Theorem 3.1 *Let $T = T_\tau$ be a transfer operator for lag time $\tau > 0$ with properties as described above, in particular (5), (6), (10), and (11). Let the disjoint sets A_1, \dots, A_n form a full partition and define*

$$\|Q^\perp u_j\| =: \delta_j \leq 1 \quad \forall j, \quad \delta(A) := \max_{j=1, \dots, m} \delta_j \quad (21)$$

where $Q^\perp = \text{Id} - Q$ denotes the projection onto the orthogonal complement of D_n in L_μ^2 . Furthermore set

$$\eta(\tau) := \frac{r}{\lambda_1} = \exp(-\tau\Delta) < 1, \quad \text{with } \Delta > 0.$$

Then the error (19) is bounded from above by

$$E(k) \leq \min \left[2; C(\delta(A), \eta(\tau), k) \right] \cdot \lambda_1^k, \quad (22)$$

with a leading constant of following form

$$C(\delta, \eta, k) = (m\delta + \eta) \left[C_{\text{sets}}(\delta, k) + C_{\text{spec}}(\eta, k) \right] \quad (23)$$

$$C_{\text{sets}}(\delta, k) = m^{1/2}(k-1)\delta \quad (24)$$

$$C_{\text{spec}}(\eta, k) = \frac{\eta}{1-\eta}(1-\eta^{k-1}). \quad (25)$$

The proof can be found in Section 6.2.

3.3 Interpretation and Observations

The theorem shows that the overall error can be made arbitrarily small by making the factor $[C_{\text{sets}}(\delta, k) + C_{\text{spec}}(\eta, k)]$ small. In order to understand the role of these two terms, consider for now the time of interest to be fixed at some $k \geq 2$. It can then be observed that:

1. The prefactor C_{sets} depends on the choice of the sets A_1, \dots, A_n only. It can be made smaller than any tolerance by choosing the sets appropriately and the number of sets, n large enough.

2. The prefactor C_{spec} is independent of the set definition and depends on the spectral gap Δ and the lag time τ only. While the spectral gap is given by the problem, the lag time may be chosen and thus C_{spec} can also be made smaller than any tolerance by choosing τ large enough. However, the factor C_{spec} will grow unboundedly for $\tau \rightarrow 0$ and $k \rightarrow \infty$, suggesting that using a large enough lagtime is essential to obtain an MSM with good approximation quality, even if the sets are well approximated.

If we are interested in a certain time scale, say T , then we have to set $k - 1 = T/\tau$. Then the pre-factor gets the form

$$C(\delta, \eta, T/\tau) = (m\delta + \eta) \left[m^{1/2} \frac{T}{\tau} \delta + \frac{\eta}{1 - \eta} F \right], \quad F = 1 - \exp(-T\Delta),$$

in which the numbers m , and T have been chosen by the user, the spectral gap Δ is determined by the $(m + 1)$ st eigenvalue and thus, for given m , a constant of the system. The error thus depends on the choice of the sets (*via* δ) and the lag time τ (and with it $\eta = \exp(-\tau\Delta)$). In the case where one is interested in the slowest process in the system, the time of interest may be directly related to the second eigenvalue *via* $T \propto 1/\Lambda_1$. For example, one may choose the half-life time of the decay of the slowest process: $T = \log 2/\Lambda_1$.

Vanishing noise diffusion. There are quite a few articles concerned with showing that a diffusion process in a multi-well landscape for vanishing noise can be approximated by a Markov jump process between the basins of the wells [4]. There the one-dimensional continuous stochastic process $(X_t)_{t \in \mathbb{R}}$ is governed by the stochastic differential equation

$$dX_t = -\nabla V(X_t)dt + \sqrt{2\epsilon}dB_t, \quad (26)$$

where B_t denotes standard Brownian motion, $\sqrt{2\epsilon}$ the small noise intensity and V the potential as, e.g., illustrated in Figure 1.

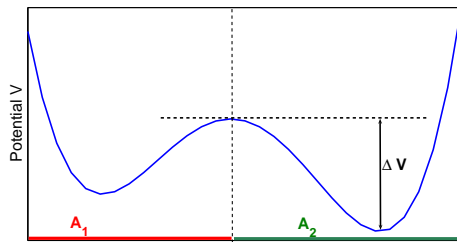


Fig. 1 The double well potential V .

The associated process satisfies our assumptions on the transfer operator. In particular, the transfer operator is self-adjoint such that the spectrum is real-valued and we have $\Lambda_1 \propto \exp(-\Delta V/\epsilon)$. As $\epsilon \rightarrow 0$, we have $\Delta = \mathcal{O}(1)$ while the timescale of interest increases exponentially, $T \propto \exp(\Delta V/\epsilon)$. Taking $m = 1$, it is indeed found that the projection error δ , with sets A_1, A_2 chosen as shown in Figure 1, also decreases exponentially with ϵ : As shown in Ref. [17], there is a $0 < v < \Delta V$ such that $\delta \propto \exp(-v/\epsilon)$. When choosing the lag time τ such that it decreases exponentially with $\epsilon \rightarrow 0$, $\tau \propto \exp(-\xi/\epsilon)$ with $\xi > \max(\Delta V - 2v, 0)$, then the upper bound E on the approximation error decreases exponentially with ϵ ,

$$E(T) \propto \exp((\Delta V - 2v - \xi)/\epsilon), \quad \text{with } \Delta V - 2v - \xi > 0.$$

Note that the fraction T/τ still grows exponentially with the vanishing noise, i.e. the time resolution of the MSM improves drastically compared to the timescale of interest. If $v > \Delta V/2$, τ can even be on the order of $1/\epsilon$ while still retaining an exponentially vanishing error.

Bounding the error. Consider that the desired quality of the MSM approximation is defined by the user *via* some tolerable error bound tol at some timescale T . This requirement is met by satisfying $E(T) \leq tol$. A rational procedure for guaranteeing this can be outlined as follows:

1. Define the timescale of interest, T .
2. Define the number of eigenfunctions, m , that we are seeking to approximate well.
3. Compute the spectral gap, Δ , which is ideally given by the $(m + 1)$ st eigenvalue. This will be directly accessible only for simple systems. For more complex systems, it may however be possible to bound Δ from below and thus guarantee that $E(k)$ remains an upper bound. In practical cases involving statistical uncertainty (e.g. molecular dynamics), one may only be able to estimate a probability distribution of the eigenvalues and thus, for any given dataset, be able to specify a Δ that the real spectral gap is *almost certainly* larger.
4. Set the desired lag time, τ depending on how much time resolution is desired compared to the time scale of interest.
5. Solve

$$tol = (m\delta + \eta) \left(m^{1/2} \delta \frac{T}{\tau} + \frac{\eta}{1 - \eta} F \right), \quad \text{with } \eta = \exp(-\tau\Delta), \text{ and } F = 1 - \exp(-T\Delta). \quad (27)$$

for δ and adapt the choice of the sets A_1, \dots, A_n and their number n to the requirement $\delta = \delta(\tau)$ as it results from (27). We will illustrate this in an explicit example in Section 5.

For practical applications, δ can also only be estimated and an approach to do this based on two differently fine discretizations is outlined in Sec. 4.3 below

Metastability. [3] gives the following theorem in which smallness of the projection error δ is related to the metastability of a subdivision A_0, \dots, A_m of state space:

Theorem 3.2 *Let T be a self-adjoint transfer operator with lag time τ and properties as described above, in particular (5), (6), (10), and (11). The metastability of an arbitrary decomposition A_0, \dots, A_m of the state space is bounded from below and above by*

$$1 + (1 - \delta_1^2)\lambda_1 + \dots + (1 - \delta_m^2)\lambda_m + c \leq \sum_{j=1}^m \mathbb{P}_\mu[X_\tau \in A_j | X_0 \in A_j] \leq 1 + \lambda_1 + \dots + \lambda_m,$$

where, as above, $\delta_j = \|Q^\perp u_j\|$, and $c = -r(\delta_1^2 + \dots + \delta_m^2)$.

This result tells us that the minimization of δ with $m + 1$ sets (for $m + 1$ eigenvalues) corresponds to identifying the subdivision with maximum joint metastability.

3.4 Generalization of the projection Q

Thm. 3.1 can easily be generalized. Firstly, we can easily see that we do not need to assume that the dynamical process (X_t) under consideration is time-continuous. Our results still hold, if $T = T_\tau$ denote the transfer operator for τ steps of some time-discrete process, and the lag time is no longer a continuous but a discrete variable.

It is not required that Q is the projection onto some space spanned by indicator functions. Q can be any orthogonal projection onto some linear subspace D of L_μ^2 with the property $Q\mathbf{1} = \mathbf{1}$, i.e., $\mathbf{1} \in D$:

Theorem 3.3 *Let $T = T_\tau$ be a transfer operator for lag time $\tau > 0$ with properties as described above, in particular (5), (6), (10), and (11). Let Q denote the projection onto some linear subspace D of L_μ^2 and define*

$$\|Q^\perp u_j\| =: \delta_j \leq 1 \quad \forall j, \quad \delta(A) := \max_{j=1, \dots, m} \delta_j \quad (28)$$

where $Q^\perp = \text{Id} - Q$. Define the projected transfer operator $P = QTQ$. Furthermore set $\eta(\tau) = \exp(-\tau\Delta) < 1$ with $\Delta > 0$. Then the error $E(k) = \|QT^kQ - P^k\|$ is bounded from above by

$$E(k) \leq \min \left[2; C(\delta(A), \eta(\tau), k) \right] \cdot \lambda_1^k, \quad (29)$$

where $C(\delta, \eta, k)$ is as in Thm. 3.1.

Note that in this general case P does not necessarily have the interpretation of a transition matrix. For this, consider the following two examples:

1. Let us decompose state space into two components, $E = E_x \times E_y$, such that every $z \in E$ can be written $z = (x, y)$ with $x \in E_x$, $y \in E_y$. We consider the (infinite dimensional) subspace

$$D = \{g \in L_\mu^2 : g(x, \cdot) \text{ is constant on } E_y \text{ for all } x \in E_x\},$$

and

$$Qv(x) = \int_{E_y} v(x, y) \mu_x(dy), \quad (30)$$

where $\mu_x(C) = \int_C \mu(x, dy) / \int_{E_y} \mu(x, dy)$ is the marginal of the invariant measure for fixed x . Associated averaged transfer operators are considered in the context of so-called Hybrid Monte Carlo methods, see [3, 2].

2. Consider the same projection Q as in Eq. (30) above, with $E_x = \text{span}\{u_0, \dots, u_m\}$, i.e. the projection onto the m -dimensional slow subspace of the dynamics. For this case, the MSM error $E(k)$ is 0 for all k , showing that a Markovian formulation of the dynamics in the slow subspace is in principle possible. In practical applications, however, it is often desired to obtain equations of motion in a subspace spanned by some slow intrinsic degrees of freedom of the system, which usually do not perfectly lie in $\text{span}\{u_0, \dots, u_m\}$, such that there is still a finite projection error remaining.
3. Instead of the indicator functions we may choose mollified indicator functions $f_j \geq 0$, $j = 1, \dots, n$. Then $D = \text{span}\{f_1, \dots, f_n\}$ but the ansatz function may no longer be orthogonal such that we have to consider the mass matrix M with entries $M_{ij} = \langle f_i, f_j \rangle$. Then,

$$Qv = \sum_{i,j=1}^n (M^{-1})_{ij} \langle f_j, v \rangle f_i. \quad (31)$$

Such mollified or fuzzy MSM have been considered, e.g., in [23] (see Section 4.1 below).

4 Algorithmic Considerations

4.1 Almost exact fuzzy MSM

Let us return to the last example of generalization in Sec. 3.4. There, the MSM subspace spanned by the indicator function of sets has been replaced by another finite dimensional subspace, $D = \text{span}\{f_1, \dots, f_n\}$, with ansatz functions that no longer are indicator functions. Now, assume that we can design (almost everywhere) non-negative ansatz function by linear combination of the eigenvector u_j , i.e.,

$$f_j = \sum_{k=0}^m a_{jk} u_j, \quad \text{with scalars } a_{jk} \text{ for } j = 0, \dots, m.$$

Then, by construction, we have that $D = \text{span}\{f_0, \dots, f_m\} = U$ and $\mathbf{1} \in D$ such that Theorem 3.3 applies with projection error $\delta = 0$. This results in a fuzzy MSM with transfer operator $P = QTQ$ with

Q according to (31); obviously P can no longer be interpreted as a transition matrix between sets in state space. In addition to $\delta = 0$ we also have $\Pi = Q$ in the proof of Thm. 3.1. This implies immediately that

$$E(k) = \|QT^kQ - P^k\| = 0, \quad \forall k = 1, 2, 3, \dots,$$

showing that the MSM is exact. M. Weber et al have developed such an MSM variant and discussed its applicability and interpretation [23]; in particular they show how to optimally compute the coefficients a_{ij} for non-negative fuzzy membership functions [24]. A warning seems appropriate: The exactness requires to have the eigenvectors of T exactly. This is something that cannot be assumed in practice: the eigenvectors result from numerical computations and will be effected by statistical and numerical errors. Thus, any practical implementation of this strategy will also have to consider the actual approximation quality of the MSM depending on the δ induced by the numerical approximation of the f_i and on the lagtime τ .

4.2 MSM based on projections of the original dynamics

In practice, MSMs are often constructed not by considering arbitrary sets $A_j \subset E$ but only sets which result from discretization of the subspace of a certain set of “essential” coordinates $\theta : E \rightarrow \theta(E) \subset E$. For example, in molecular systems, one usually ignores the solvent coordinates [8, 25, 6] and may even further only consider a subset of solute coordinates such as torsion angles [25, 6]. The projection of the original process on the essential subspace, $\theta(X_t)_{t \in R}$, will then in general be far from being Markovian. However, this does not concern our result or the construction of MSM in general. Let $E(A) = \{x \in E : \theta(x) \in A\}$ denote the cylinder set that belongs to a subset A of the essential subspace $\theta(E)$. Thus, any subdivision A_1, \dots, A_n of $\theta(E)$ will induce a subdivision $E(A_1), \dots, E(A_n)$ of the full state space E . Thus, the above results are fully valid if applied to these subdivisions. So the question of whether an MSM based on a definition of states in a subspace θ has good approximation quality boils down to the question of whether the projection error δ can be kept below a certain accuracy threshold based on cylinder sets. A necessary condition for this possibility is that the eigenvectors u_0, \dots, u_m of the original transfer operator in full state space E are almost constant along the fibers $E(\vartheta) = \{x \in E : \theta(x) = \vartheta\}$. In other words, the approximation quality of the MSM can be good if the variables ignored by the projection onto θ are sufficiently fast.

4.3 Comparing coarser and finer MSM

In practical cases, the eigenvectors and eigenvalues of T are not directly available. Because of that many articles in the MSM literature consider a fine subdivision of the state space and the associated MSM first and construct the final, coarse MSM based on the eigenvectors and -values of the fine MSM [2, 26, 8, 5, 6]. In order to analyse this procedure based on the above estimate of the MSM error, let us consider a case with two subdivisions of very different fineness,

$$\begin{aligned} A_1^{(1)}, \dots, A_N^{(1)} & : \text{ fine subdivision of } E, \\ A_1^{(2)}, \dots, A_n^{(2)} & : \text{ coarse subdivision of } E, \quad n \ll N, \end{aligned}$$

consider the associated projections

$$\begin{aligned} Q^{(1)} & : \text{ fine grid orthogonal projection} \\ Q^{(2)} & : \text{ coarse grid orthogonal projection} \\ Q^{(12)} & : \text{ fine to coarse orthogonal projection.} \end{aligned}$$

and the induced MSM transfer operators

$$\begin{aligned} P^{(1)} = Q^{(1)}TQ^{(1)} & : \text{ transfer operator of fine MSM process} \\ P^{(2)} = Q^{(2)}TQ^{(2)} & : \text{ transfer operator of coarse MSM process.} \end{aligned}$$

Obviously the projection error of the eigenvectors of T can be quite different:

Lemma 4.1 *The fine and coarse projection error,*

$$\delta^{(1)} = \max_j \|Q^{(1),\perp} u_j\|, \quad \delta^{(2)} = \max_j \|Q^{(2),\perp} u_j\|,$$

and the errors of the fine and coarse MSM satisfy the estimate

$$\begin{aligned} \delta^{(2)} - \delta^{(1)} &\leq \delta^{(12)} \\ (\delta^{(2)})^2 - (\delta^{(1)})^2 &\leq (\delta^{(12)})^2 \\ E_2(k) - E_1(k) &\leq \|Q^{(12)}(P^{(1)})^k Q^{(12)} - (P^{(2)})^k\|, \end{aligned}$$

where $\delta_j^{(12)} = \|Q^{(12),\perp} Q^{(1)} u_j\|$, and the last norm has to be evaluated on $\text{Range}(Q^{(1)}) = \text{span}\{\chi_{A_j}, j = 1, \dots, n\}$.

The proof of this lemma is given in Sec. 6.3 below.

This Lemma makes explicit that coarse-graining the state definition via $Q^{(12)}$ will always increase the MSM error, as long as statistical effects are not considered.

4.4 Statistical and total error

When considering MSM for biomolecular systems the MSM transfer operator P or its matrix representation (P_{ij}) are normally not known exactly. Instead, only statistical approximations \tilde{P}_{ij} of its entries

$$\tilde{P}_{ij} \approx \mathbb{P}_\mu(X_\tau \in A_j | X_0 \in A_i).$$

are available. Thus, the total error of an MSM compared to the original dynamics is not $E(k) = \|QT^k Q - P^k\|$ but

$$\tilde{E}(k) = \|QT^k Q - \tilde{P}^k\| \leq E(k) + \|P^k - \tilde{P}^k\|.$$

There are several approaches to estimation of the *statistical error* $\|P^k - \tilde{P}^k\|$ [27, 28, 29]. So it seems that combining these approaches to the results presented herein should give control of the total error \tilde{E} . However, a warning seems appropriate: Being able to bound E via Theorem 3.1 requires knowledge of P instead of \tilde{P} such that additional research will be needed to be able to bound the total error.

5 Numerical Examples

5.1 Double well potential

The results and concepts from above will first be illustrated on a one-dimensional diffusion in a double-well potential. In contrast to the diffusive dynamics considered in Sec. XX above, this example does not rely on vanishing noise approximations but considers the process $dX_t = -\nabla V(X_t)dt + \sigma dB_t$ with some $\sigma > 0$. The potential V and its unique invariant measure is shown in Fig.2.

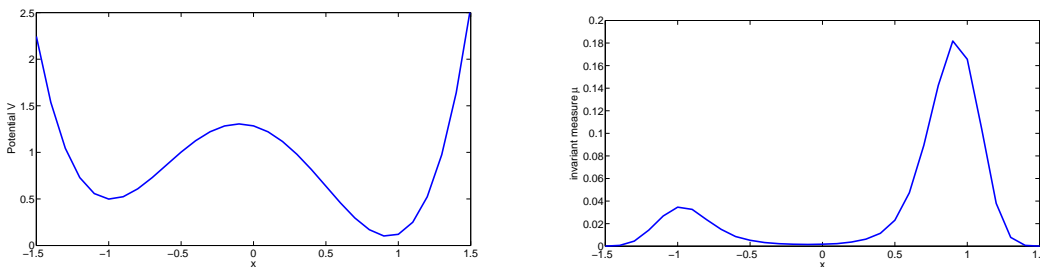


Fig. 2 (a) The potential V and (b) the associated invariant measure.

This process satisfies all necessary assumptions and by resolving only the slowest process ($m = 1$), the following spectral values are obtained:

$$\Lambda_1 = 0.201, \quad R = 16.363, \quad \Delta = 16.162.$$

The eigenvector u_1 is given in the middle panel of Figure 3; It is seen that it is almost constant on the two wells of the potentials and changes sign close to where its saddle point is located.

Projection error δ . Let us first choose the lag time $\tau = 0.1$. Then $\lambda_1 = 0.9801$ and $r = 0.1947$. Fig. 3 shows the values of the projection error δ for $n = 2$ and sets of the form $A_1 = (-\infty; x]$ and $A_2 = (x; \infty)$ depending on the position of the dividing surface, x . One can see that it is optimal for

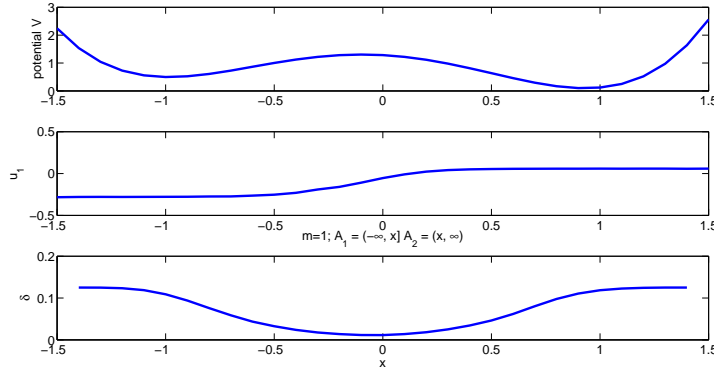


Fig. 3 Upper panel: Potential V . Middle panel: Eigenvector u_1 . Lower Panel: Projection error δ for different sets $A_1 = (-\infty; x]$ and $A_2 = (x; \infty)$ plotted against x .

the boundary between the two sets to lie close to the saddle point of the potential, where the second eigenvector is strongly varying.

Next let us study the effect of different discretizations/partitioning of state space on δ . First, A_1, \dots, A_n are chosen as a uniform discretization of x , the case $n = 5$ being shown in Fig.4. For

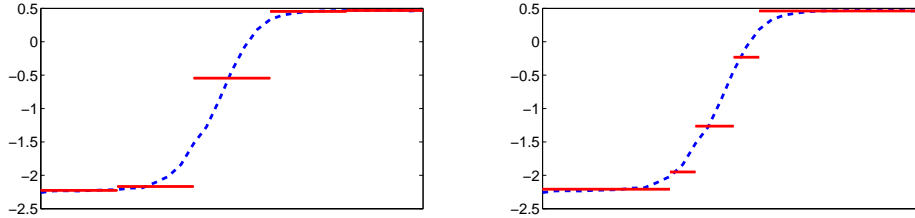


Fig. 4 Galerkin approximation Qu_1 of second eigenvector. Left panel: uniform grid of $n = 5$ sets. Right panel: Adaptive grid with $n = 5$ sets.

the uniform discretization the projection error δ does not monotonically decrease with increasing n , as shown in Fig. 5. This means that our discrete approximation of the transfer operator can even get worse while uniformly refining the grid. Therefore using a uniform discretization should be avoided. Next, a simple adaptive refinement strategy is considered: For the case $n = 2$, the dividing surface is placed so as to minimize the δ error (see Fig. 3). For $n = 3$, another dividing surface is introduced at a point that minimized the resulting δ -error, and so on. See Figure 4 (panel) for the result for $n = 5$. While this strategy does not yield an optimal discretization for $n > 2$, it guarantees that the error decreases monotonically with increasing n , as shown in Fig. 5. Fig.4 (panel) shows that the refinement is concentrated on the transition region between the minima of the potential, since most of the projection error is made in this region resulting from the strong variation of the eigenvector.

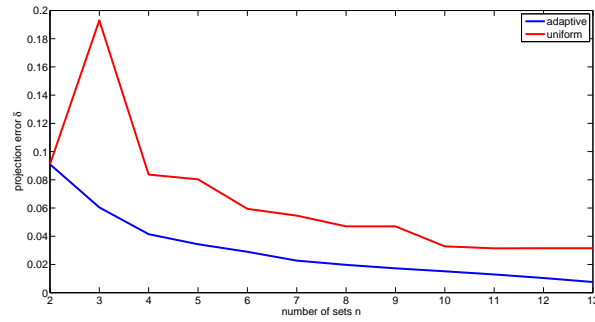


Fig. 5 Approximation error δ against number of sets n for uniform and adaptive discretization.

Effect of the lag time. Next let us study the effect of different lag times τ . For this, we fix the choice of the sets to $n = 3$ adaptive sets. Figs. 6 and 8 show the bound on the MSM approximation error $E(k)$ from Theorem 3.1 compared to the exact approximation error $E(k)$ computed via extensive direct numerical simulation. Upon increasing the lag time from $\tau = 0.1$ to $\tau = 0.5$ the bound from

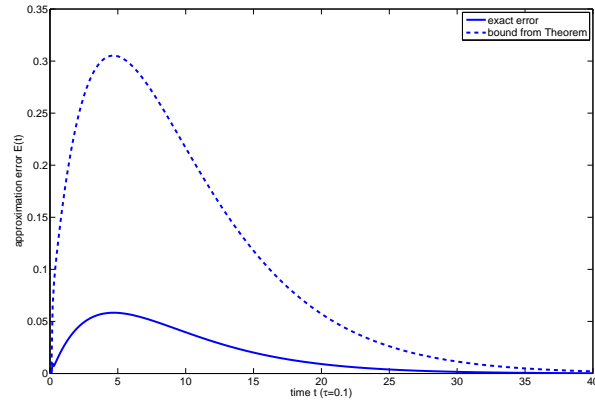


Fig. 6 Bound and exact error E for $\tau = 0.1$ on adaptive grid with $n = 3$ adaptive sets.

Theorem 3.1 becomes much sharper, see Fig. 7. Secondly, the approximation quality of the MSM becomes significantly better when the lag time is increased. Finally, Fig. 9 compares exact errors and bounds for $n = 3$ sets with uniform and adaptive grid with lag time $\tau = 0.5$ exhibiting a dramatic advantage of the adaptive over the uniform discretization for longer lag times.

Number of sets necessary to yield a given error and lag time. Let us shortly come back to the question how to build an MSM if the maximum acceptable approximation error tol is given. In the present case, Δ is known explicitly. Thus, as explained in Sec.3.3, for a given lag time τ the value of δ that is required for $E(T) = \text{tol} = 0.1$ can be computed (Fig. 10, solid line). Next, we consider the adaptive discretization with $n = 2, 3, 4, \dots$ and compute their δ -error (Boxes in Fig. 10). This shows that the required error tolerance of 0.1 can be obtained with different n - τ pairs, e.g. using $n = 2$ with $\tau \approx 0.3$ or $n = 5$ with $\tau \approx 0.15$.

5.2 Double well potential with diffusive transition region

Let us now consider a one-dimensional diffusion in a different potential with two wells that are connected by an extended transition region with substructure: $dX_t = -\nabla V(X_t)dt + \sigma dB_t$ with $\sigma = 0.8$. The

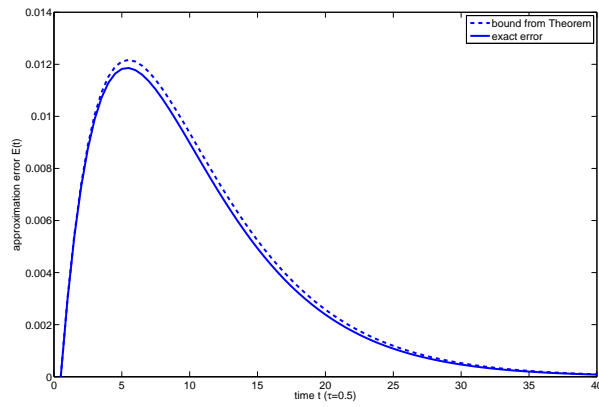


Fig. 7 Bound and exact error E for $\tau = 0.5$ on adaptive grid with $n = 3$.

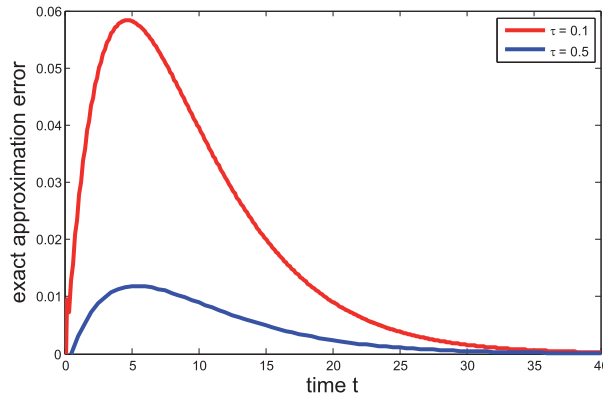


Fig. 8 Exact error E for different lag times ($\tau = 0.1$ and 0.5) on adaptive grid with $n = 3$.

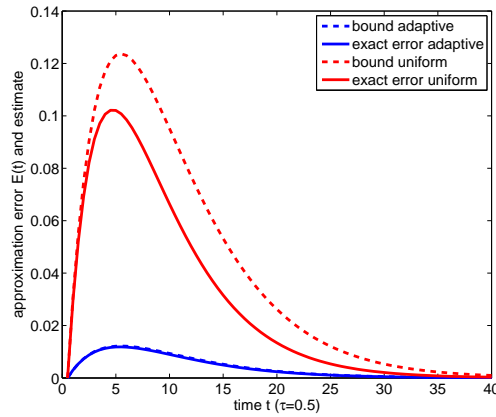


Fig. 9 Exact error and bound for uniform and adaptive grid, $n = 3$, $\tau = 0.5$.

potential V and its unique invariant measure are shown in Fig.11. We observe that the transition region between the two main wells now contains four smaller wells that will have their own, less pronounced metastability each. When considering the semigroup of transfer operators associated with this dynamics

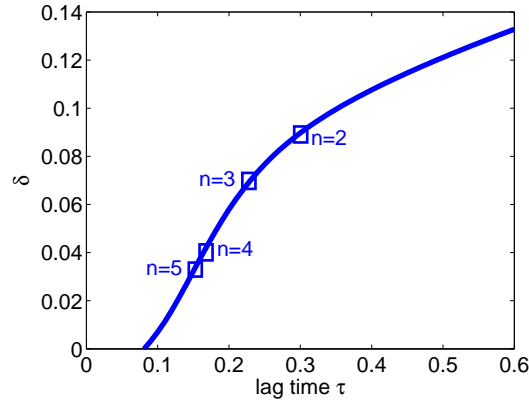


Fig. 10 Dependence of the requirement for δ on τ for prescribed error $\text{tol} = 0.1$. The boxes indicate some values of δ that can be realized by choosing n adaptive boxes.

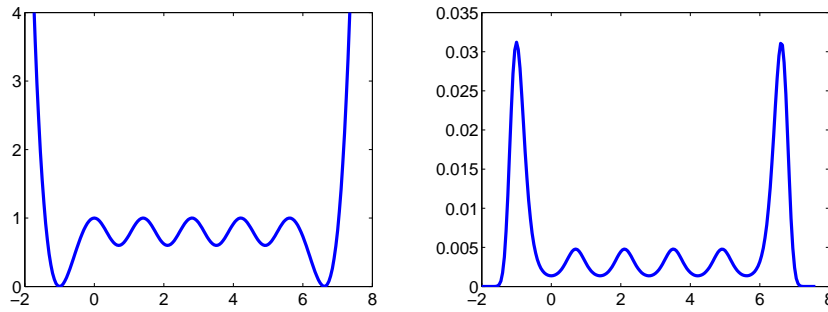


Fig. 11 The potential V with extended transition region and the associated invariant measure for $\sigma = 0.8$.

we find the dominant eigenvectors as shown in Fig. 12. The eigenvectors all are almost constant on the two main wells but are non-constant in the transition region. The dominant eigenvalues take the following values (in the form of lagtime-independent rates as introduced above):

$$\begin{array}{cccccccc} \Lambda_0 & \Lambda_1 & \Lambda_2 & \Lambda_3 & \Lambda_4 & \Lambda_5 & \Lambda_6 & \Lambda_7 \\ +0.0000 & -0.0115 & -0.0784 & -0.2347 & -0.4640 & -0.7017 & -2.9652 & -3.2861 \end{array}$$

The main metastability has a corresponding timescale $|1/\Lambda_1| \approx 87$ related to the transitions from one of the main wells to the other. Four other, minor metastable timescales related to the interwell switches between the main and the four additional small wells exist in addition.

Adaptive subdivisions and projection error. Let us first fix $m = 2$ and lagtime $\tau = 0.5$ and study how the decay of the projection error depends on the number n of sets in the respective optimal adaptive subdivision. To this end we first observe that adaptive subdivisions will have to decompose the transition regions finer and finer, see Figure 13 for an example for $n = 20$. The decay of the projection error δ with n is shown in Figure 14. Figure 14 also includes the comparison of the decay of δ with n and the decay of the total propagation error of the underlying MSMs. We observe that the two curves decay in a similar fashion as suggested by our error bound E on the propagation error.

The role of m and lagtime τ . There is a trade-off between the projection error δ and the spectral part of the error that can be modulated by varying the number of resolved eigenfunctions, m . When increasing m , more eigenvectors are taken into account and the minimal projection error that can be

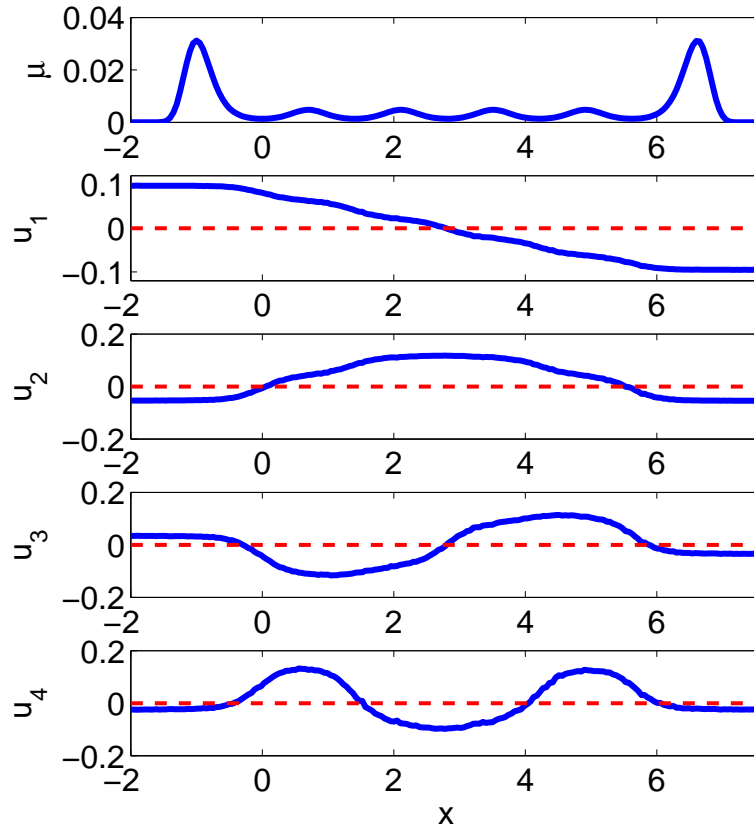


Fig. 12 Invariant measure and eigenvectors u_j , $j = 1, \dots, 4$ for Brownian motion in the potential V with extended transition region from Figure 11 for $\sigma = 0.8$.

obtained with a fixed number of stepfunctions, n , will increase. On the other hand, the spectral part of the error will decrease as growing m increases the spectral gap Δ . This means that increasing m and thus Δ will allow to decrease the lagtime τ without changing the spectral error.

In order to understand how strongly the projection error δ depends on m we show the dependence of δ on m and the number n adaptively chosen sets in Figure 15. We observe that the increase of m for fixed n is significant but not dramatic. Let us next assume that we want to guarantee that the total propagation error is below 0.1 for all times k . Then, a certain choice of m and n fixes Δ and δ and allows the minimal lagtime τ_* to be computed that is required to guarantee $\max_k E(k) \leq 0.1$. Figure 16 shows how τ_* depends on m and n . It is observed that $m = 2$ yields the best results, that is, for given n the lagtime can be chosen smallest with $m = 2$ in comparison to $m = 1$ and $m = 5$ (and other values of m not shown in the last figure).

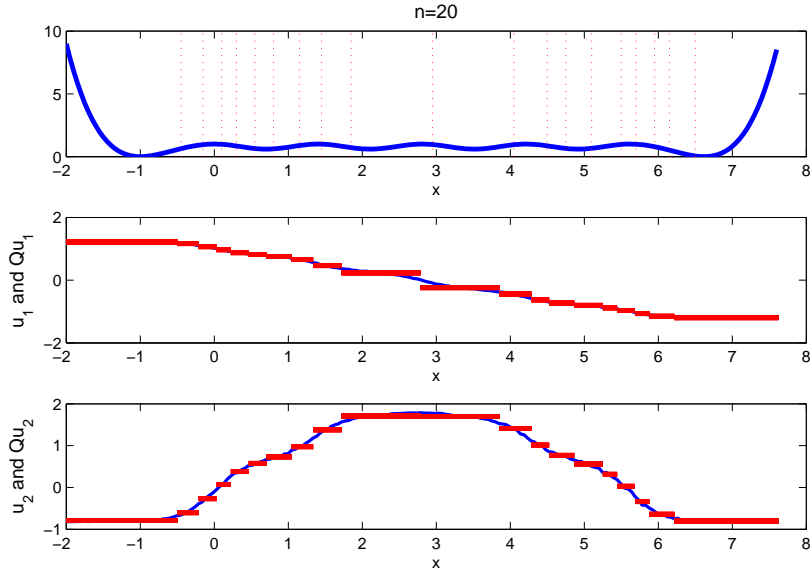


Fig. 13 Potential and eigenvectors u_j , $j = 1, 2$ and their stepfunction approximation Qu_j for $n = 20$ adaptive sets. The resulting projection error is $\delta = 0.052$.

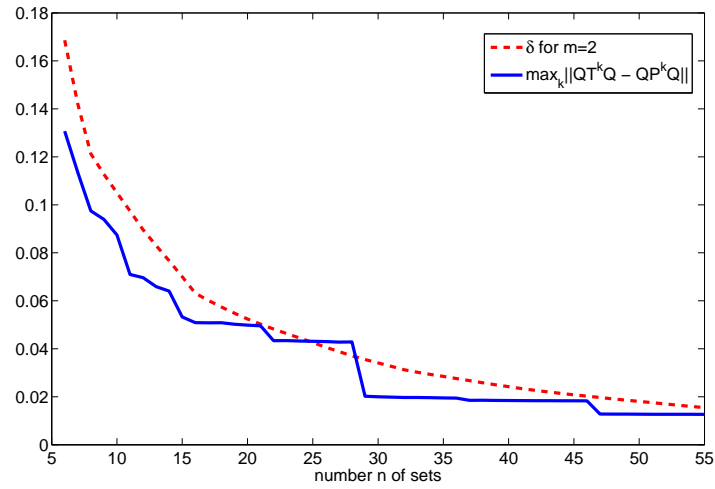


Fig. 14 Decay of δ and of the maximal propagation error $\max_k \|QT^k Q - P^k\|$ with the number n of sets in the optimal adaptive subdivision for $m = 2$.

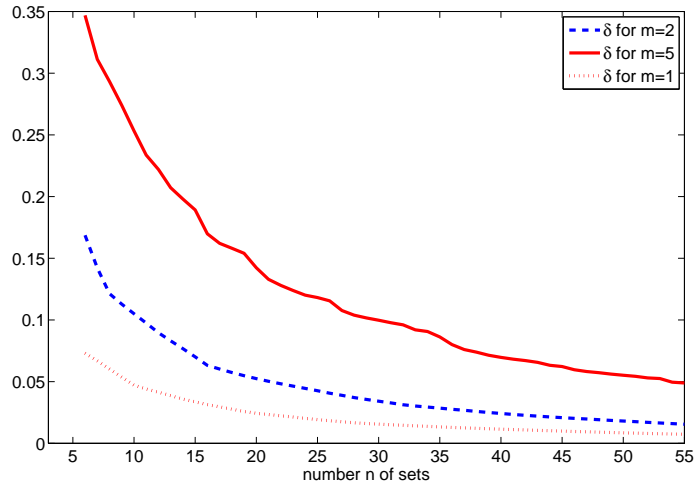


Fig. 15 Decay of δ with the number n of sets in the optimal adaptive subdivision for $m = 1, 2, 5$.

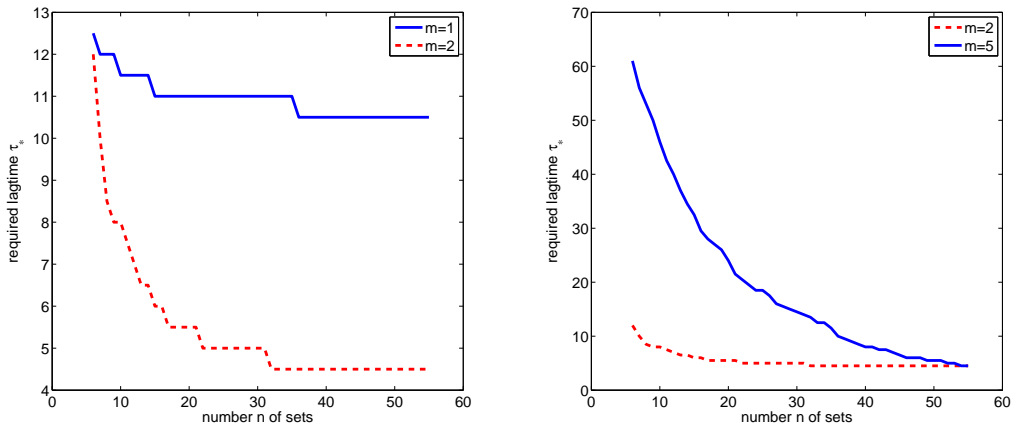


Fig. 16 Comparison of the minimal lagtime τ_* that is required to achieve $\max_k E(k) \leq 0.1$ depending on the number n of sets in the optimal adaptive subdivision. Right hand panel: $m = 1$ compared to $m = 2$. Left panel: $m = 2$ compared to $m = 5$.

6 Proofs

6.1 Proof of Lemma 2.2.

Proof. Because of $\Pi_0 Q = Q \Pi_0 = \Pi_0$ and $\|T - \Pi_0\| = \lambda_1$ we have for $k = 1$:

$$\|TQ - \Pi_0\| = \|(T - \Pi_0)Q\| \leq \lambda_1. \quad (32)$$

Since furthermore $T\Pi_0 = \Pi_0$, and $T\Pi$ is self-adjoint we find for arbitrary $v \in L_\mu^2$:

$$\begin{aligned} \Pi_0 T v &= \langle T v, \mathbf{1} \rangle \mathbf{1} = \langle T \Pi v, \mathbf{1} \rangle \mathbf{1} + \langle T \Pi^\perp v, \Pi \mathbf{1} \rangle \mathbf{1} \\ &= \langle v, T \Pi \mathbf{1} \rangle \mathbf{1} + \langle \Pi T \Pi^\perp v, \mathbf{1} \rangle \mathbf{1} = \langle v, \mathbf{1} \rangle \mathbf{1} = \Pi_0 v, \end{aligned}$$

where the identity before the last follows from (11). Therefore

$$\Pi_0 T = T \Pi_0 = \Pi_0. \quad (33)$$

From this and $Q \Pi_0 = \Pi_0 Q = \Pi_0$ it follows that $(TQ - \Pi_0)^k = (TQ)^k - \Pi_0$ and thus with (32)

$$\|P^k - \Pi_0\| = \|Q(TQ)^k - Q \Pi_0\| \leq \|(TQ)^k - \Pi_0\| = \|(TQ - \Pi_0)^k\| \leq \|TQ - \Pi_0\|^k \leq \lambda_1^k,$$

which was the assertion. \square

6.2 Proof of Theorem 3.1

First we observe that the error in (19) at time k consists of the $k-1$ projection errors that are propagated until time k is reached, as direct calculation shows:

$$QT^k Q - QP^k Q = \sum_{i=1}^{k-1} QT^i Q^\perp (TQ)^{k-i}.$$

By this expression we can estimate the approximation error E by observing that it consists of two different parts. Because of $Q^\perp Q^\perp = Q^\perp$ we have

$$\|QT^k Q - QP^k Q\| \leq \sum_{i=1}^{k-1} \|QT^i Q^\perp\| \|Q^\perp (TQ)^{k-i}\|. \quad (34)$$

The first term $\|QT^i Q^\perp\|$ describes the propagation of the projection error in i steps and the second term $\|Q^\perp (TQ)^{k-i}\|$ measures how large a projection error can be in the $(k-i)$ -th iteration of applying operator P . So the i -th summand explains the effect of propagation of error that is made in the $(k-i)$ -th iteration.

We will estimate the overall error by looking at both parts of error separately. Let us prepare this with the following lemma:

Lemma 6.1 *For the first part of the error we have the upper bound*

$$\|QT^k Q^\perp\| \leq \sqrt{m} \lambda_1^k \delta + r^k.$$

Proof. Let v be arbitrary with $\|v\| = 1$. Because $u_0 = \mathbf{1}$ and $Q^\perp u_0 = 0$,

$$(T\Pi)^k Q^\perp v = T^k \Pi Q^\perp v = \sum_{j=1}^m \lambda_j^k \langle Q^\perp u_j, v \rangle u_j,$$

which leads to

$$\|(T\Pi)^k Q^\perp v\|^2 = \sum_{j=1}^m \lambda_j^{2k} \langle Q^\perp u_j, v \rangle^2 \stackrel{(21)}{\leq} m \lambda_1^{2k} \delta^2.$$

and therefore

$$\|Q(T\Pi)^k Q^\perp\| \leq \sqrt{m}\lambda_1^k \delta. \quad (35)$$

Now we can estimate

$$\|QT^k Q^\perp\| \stackrel{(12)}{\leq} \|Q(T\Pi)^k Q^\perp\| + \|Q(T\Pi^\perp)^k Q^\perp\| \stackrel{(35)}{\leq} \sqrt{m}\lambda_1^k \delta + \|T\Pi^\perp\|^k \stackrel{(10)}{\leq} \sqrt{m}\lambda_1^k \delta + r^k. \quad (36)$$

□

Now we can proof Theorem 3.1.

Proof. First recall that the first argument 2 in the minimum taken in (22) comes from (20). Moreover, recall (34), that is,

$$\|QT^k Q - QP^k Q\| \leq \sum_{i=1}^{k-1} \|QT^i Q^\perp\| \|Q^\perp(TQ)^{k-i}\|.$$

Because $Q^\perp \Pi_0 = 0$ we can write

$$\|Q^\perp(TQ)^{k-i}\| = \|Q^\perp TQ(TQ)^{k-i-1}\| = \|Q^\perp TQ((TQ)^{k-i-1} - \Pi_0)\|.$$

Moreover

$$\|Q^\perp TQ\| \leq \|Q^\perp T\Pi Q\| + \|Q^\perp T\Pi^\perp Q\| \leq \|Q^\perp T\Pi Q\| + r$$

and for v with $\|v\| = 1$

$$\|Q^\perp T\Pi Q v\|^2 = \sum_{i,j=1}^m \langle Qv, u_i \rangle \langle Qv, u_j \rangle \lambda_i \lambda_j \langle Q^\perp u_i, Q^\perp u_j \rangle \leq m^2 \lambda_1^2 \delta^2 \|v\|^2.$$

We use Lemma 2.2 to get

$$\|Q^\perp TQ((TQ)^{k-i-1} - \Pi_0)\| \leq (m\lambda_1 \delta + r)\lambda_1^{k-i-1}. \quad (37)$$

Inserting (37) and Lemma 6.1 into (34) yields

$$E(k) = \|QT^k Q - Q(TQ)^k\| \leq (m\lambda_1 \delta + r) \sum_{i=1}^{k-1} (\sqrt{m}\lambda_1^i \delta + r^i)\lambda_1^{k-i-1}.$$

Now we have

$$\sum_{i=1}^{k-1} (\sqrt{m}\lambda_1^i \delta + r^i)\lambda_1^{k-i-1} = \sqrt{m}\delta(k-1)\lambda_1^{k-1} + \lambda_1^{k-1} \sum_{i=1}^{k-1} \eta^i$$

and

$$\sum_{i=1}^{k-1} \eta^i = \frac{1-\eta^k}{1-\eta} - 1 = \frac{\eta-\eta^k}{1-\eta} = \frac{\eta}{1-\eta}(1-\eta^{k-1}).$$

□

6.3 Proof of Lemma 4.1

Remember that $Q^{(1)}$, $Q^{(2)}$ denote the projection from L_μ^2 to the fine and coarse stepfunction spaces, while $Q^{(12)}$ denotes the projection from fine to coarse.

Proof. We first find easily that $Q^{(2)} = Q^{(12)}Q^{(1)}$, and $Q^{(2),\perp} = Q^{(1),\perp} + Q^{(12),\perp}Q^{(1)}$. Setting $\delta_j^{(12)} = \|Q^{(12),\perp}Q^{(1)}u_j\|$ this implies:

$$\begin{aligned} (\delta_j^{(2)})^2 = \|Q^{(2),\perp}u_j\|^2 &= \langle (Q^{(1),\perp} + Q^{(12),\perp}Q^{(1)})u_j, (Q^{(1),\perp} + Q^{(12),\perp}Q^{(1)})u_j \rangle \\ &= \|Q^{(1),\perp}u_j\|^2 + \|Q^{(12),\perp}Q^{(1)}u_j\|^2 + 2\langle Q^{(12),\perp}Q^{(1)}u_j, Q^{(1),\perp}u_j \rangle \\ &= (\delta_j^{(2)})^2 + (\delta_j^{(12)})^2, \end{aligned}$$

where the last identity follows from the fact that $Q^{(1),\perp}Q^{(12)} = 0$ on $\text{Range}(Q^{(1)})$ which implies $Q^{(1),\perp}Q^{(12),\perp} = Q^{(1),\perp}$. The above identity implies the assertions concerning the δ -estimates. With respect to the estimate on the error it suffices to observe that

$$\begin{aligned} E_2(k) &= \|Q^{(2)}T^kQ^{(2)} - (P^{(2)})^k\| = \|Q^{(12)}Q^{(1)}T^kQ^{(12)}Q^{(1)} - (P^{(2)})^k\| \\ &= \|Q^{(12)}Q^{(1)}T^kQ^{(1)}Q^{(12)}Q^{(1)} - (P^{(2)})^k\| \\ &\leq \|Q^{(12)}Q^{(1)}T^kQ^{(1)}Q^{(12)}Q^{(1)} - Q^{(12)}(P^{(1)})^kQ^{(12)}Q^{(1)}\| \\ &\quad + \|Q^{(12)}(P^{(1)})^kQ^{(12)}Q^{(1)} - (P^{(2)})^kQ^{(1)}\| \\ &\leq E_1(k) + \|Q^{(12)}(P^{(1)})^kQ^{(12)} - (P^{(2)})^k\| \end{aligned}$$

where the last norm has to be evaluated on $\text{Range}(Q^{(1)}) = \text{span}\{\chi_{A_j}, j = 1, \dots, n\}$ which comes from ignoring the $Q^{(1)}$ in the last step of the estimate. \square

7 Conclusion

We have presented a rigorous upper bound to the error in the propagation of functions in state space between an ergodic dynamical process and a MSM based on a complete partitioning of state space.

We have demonstrated that this error mainly depends on two components: (1) the projection error associated with how well the discretization of state space can approximate the change of the dominant eigenfunctions of the original process, and (2) the lag time chosen in the transition matrix of the MSM. In particular, for fixed, large enough lag time, we have seen that an increasingly fine discretization of state space decreases the error *independently* of whether the original process coarse grained to the subdivision still satisfies the Markov property or not. This observation justifies the algorithmic strategy of constructing MSMs by finely partitioning state space using clustering algorithms that has been employed by several researchers in the field [6, 30, 31].

Our results also gives formal support to the practical experience that grouping discretization elements into metastable sets is a good strategy when a small MSM is desired [6, 23, 8, 1], but will nevertheless increase the approximation error of the MSM compared to the fine discretization for a given lag time τ . A given error tolerance can then again be met by further increasing τ to reduce the spectral part of the error. On the other hand, if a metastable subdivision does not yield a sufficiently low error for a desirable choice of τ , further reduction of the projection error by introducing additional refinements of the subdivision are needed. We have seen that such refinements will be at the transition regions. In contrast to the assumption that has been made in many applications of MSM, this shows that in order to improve the quality of an MSM one needs to go to a partitioning of state space that is not metastable.

Additional algorithmic questions like the the possible advantage of fuzzy memberships and the use of subdivisions based on only a subset of state space variables have also been discussed. The influence of the statistical error and possible strategies for bounding the total approximation error of the MSM was also discussed. Note that the requirement of improving the quality of the MSM by fine subdivisions of

the transition regions calls for adaptive simulation methods as the statistical sampling is typically worst in the transition regions.

Summarizing, on the one hand our analysis puts the questions concerning the approximation quality of MSM onto solid ground and the functional form of the error immediately suggests the development of adaptive algorithms for obtaining a discretization of state space such that the MSM approximation is guaranteed to stay below a user-defined tolerance. On the other hand, we could see that there are situations, such as potentials with large diffusive transition regions where the full partitioning of state space might require using too many states to be practically useful and new algorithmic strategies will be required for efficient construction of high quality MSMs.

References

- [1] P. Deuffhard, W. Huisinga, A. Fischer, and Ch. Schuette. Identification of almost invariant aggregates in reversible nearly uncoupled Markov chains. *Linear Algebra and its Applications*, 315:39–59, 2000.
- [2] Ch. Schuette, A. Fischer, W. Huisinga, and P. Deuffhard. A direct approach to conformational dynamics based on hybrid Monte Carlo. *J. Comp. Physics Special Issue on Computational Biophysics*, 151:146–168, 1999.
- [3] Ch. Schuette and W. Huisinga. Biomolecular conformations can be identified as metastable sets of molecular dynamics. In *Handbook of Numerical Analysis*, pages 699–744. Elsevier, 2003.
- [4] A. Bovier, M. Eckhoff, V. Gayrard, and M. Klein. Metastability and low lying spectra in reversible markov chains. *Comm. Math. Phys.*, 228:219255, 2002.
- [5] F. Noé and S. Fischer. Transition networks for modeling the kinetics of conformational change in macromolecules. *Curr. Opin. Struct. Biol.*, 18:154–162, 2008.
- [6] F. Noé, I. Horenko, Ch. Schuette, and J. Smith. Hierarchical analysis of conformational dynamics in biomolecules: Transition networks of metastable states. *J. Chem. Phys.*, 126:155102, 2007.
- [7] F. Noé, C. Schuette, L. Reich, and T. Weikl. Constructing the full ensemble of equilibrium folding pathways from short off-equilibrium simulations. *submitted to PNAS*, 2009.
- [8] J. Chodera, N. Singhal, V. S. Pande, K. Dill, and W. Swope. Automatic discovery of metastable states for the construction of Markov models of macromolecular conformational dynamics. *Journal of Chemical Physics*, 126, 2007.
- [9] Nicaolae V. Buchete and Gerhard Hummer. Coarse master equations for peptide folding dynamics. *Journal of Physical Chemistry B*, 112:6057–6069, 2008.
- [10] A. C. Pan and B. Roux. Building Markov state models along pathways to determine free energies and rates of transitions. *Journal of Chemical Physics*, 129, 2008.
- [11] A. Voter. Introduction to the kinetic Monte Carlo method. In *Radiation Effects in Solids*. Springer, NATO Publishing Unit, Dordrecht, The Netherlands, 2005.
- [12] M. Freidlin and A. D. Wentzell. *Random perturbations of dynamical systems*. Springer, New York, 1998.
- [13] Weinan E and E. Vanden Eijnden. Metastability, conformation dynamics, and transition pathways in complex systems. In *Multiscale Modelling and Simulation*, pages 38–65. Springer, 2004.
- [14] A. Bovier, M. Eckhoff, V. Gayrard, and M. Klein. Metastability in reversible diffusion processes. I. sharp asymptotics for capacities and exit times. *J. Eur. Math. Soc. (JEMS)*, 6:399424, 2004.
- [15] A. Bovier, V. Gayrard, and M. Klein. Metastability in reversible diffusion processes. II. precise asymptotics for small eigenvalues. *J. Eur. Math. Soc. (JEMS)*, 7:6999, 2005.
- [16] R.S. Maier and D.L. Stein. Limiting exit location distribution in the stochastic exit problem. *SIAM J. Appl. Math.*, 57, 1997.
- [17] Ilya Pavlyukevich. *Stochastic Resonance*. PhD thesis, HU Berlin, 2002.
- [18] W. Huisinga, S. Meyn, and Ch. Schuette. Phase transitions and metastability for Markovian and molecular systems. *Ann. Appl. Probab.*, 14:419458, 2004.
- [19] E. B. Davies. Spectral properties of metastable markov semigroups. *J. Funct. Anal.*, 52:315329, 1983.
- [20] Ch. Schuette. *Conformational Dynamics: Modelling, Theory, Algorithm, and Applications to Biomolecules*. Habilitation thesis, Fachbereich Mathematik und Informatik, FU Berlin, 1998.
- [21] F. Herau, M. Hitrik, and J. Sjostrand. Tunnel effect for Kramers-Fokker-Planck type operators: Return to equilibrium and applications. *International Mathematics Research Notices*, article ID rnn057, 2008.
- [22] P. Deuffhard, M. Dellnitz, O. Junge, and Ch. Schuette. Computation of essential molecular dynamics by subdivision techniques. In *Lecture Notes in Computational Science and Engineering*, volume 4, pages 98–115. Springer, 1999.
- [23] M. Weber. *Meshless Methods in conformation dynamics*. PhD thesis, FU Berlin, 2006.

- [24] P. Deuffhard and M. Weber. Robust perron cluster analysis in conformation dynamics. *Linear Algebra and its Applications*, 398 Special issue on matrices and mathematical biology:161–184, 2005.
- [25] Nicolae-Viorel Buchete and Gerhard Hummer. Peptide folding kinetics from replica exchange molecular dynamics. *Phys. Rev. E* 77, 2008.
- [26] N. Singhal Hinrichs and V. S. Pande. Bayesian metrics for the comparison of Markovian state models for molecular dynamics simulations. *RECOMB*, 2007. submitted.
- [27] Susanna Roebnitz. *Statistical Error Estimation and Grid-free Hierarchical Refinement in Conformation Dynamics*. PhD thesis, FU Berlin, 2008.
- [28] N. Singhal and V. S. Pande. Error analysis in Markovian state models for protein folding. *Journal of Chemical Physics*, 123, 2005.
- [29] F. Noé. Probability distributions of molecular observables computed from Markov models. *J. Chem. Phys.*, 128:244103, 2008.
- [30] F. Rao and A. Caffisch. The protein folding network. *J. Mol. Bio.*, 342:299–306, 2004.
- [31] S. V. Krivov and M. Karplus. Hidden complexity of free energy surfaces for peptide (protein) folding. *Proc. Nat. Acad. Sci. USA*, 101:14766–14770, 2004.